PROTEINS: Structure, Function, and Genetics 31:150–159 (1998)

Interaction of Transmembrane Helices by a Knobs-Into-Holes Packing Characteristic of Soluble Coiled Coils

Dieter Langosch[1]* **and Jaap Heringa**[2]
[1]*Department of Neurobiology, Universität Heidelberg, Heidelberg, Germany*
[2]*Division of Mathematical Biology, National Institute for Medical Research (NIMR), London, United Kingdom*

ABSTRACT **Membrane-embedded protein domains frequently exist as α-helical bundles, as exemplified by photosynthetic reaction centers, bacteriorhodopsin, and cytochrome C oxidase. The sidechain packing between their transmembrane helices was investigated by a nearest-neighbor analysis which identified sets of interfacial residues for each analyzed helix–helix interface. For the left-handed helix–helix pairs, the interfacial residues almost exclusively occupy positions *a*, *d*, *e*, or *g* within a heptad motif (*abcdefg*) which is repeated two to three times for each interacting helical surface. The connectivity between the interfacial residues of adjacent helices conforms to the knobs-into-holes type of sidechain packing known from soluble coiled coils. These results demonstrate on a quantitative basis that the geometry of sidechain packing is similar for left-handed helix–helix pairs embedded in membranes and coiled coils of soluble proteins. The transmembrane helix–helix interfaces studied are somewhat less compact and regular as compared to soluble coiled coils and tolerate all hydrophobic amino acid types to similar degrees. The results are discussed with respect to previous experimental findings which demonstrate that specific interactions between transmembrane helices are important for membrane protein folding and/or oligomerization. Proteins 31:150–159, 1998.**

Key words: photosynthetic reaction center; bacteriorhodopsin; cytochrome C oxidase; zipper; packing

INTRODUCTION

The majority of the structurally well-characterized integral membrane proteins display α-helical transmembrane (TM) segments. These TM-helices may form well-packed bundles as found in photosynthetic reaction centers,[1–3] bacteriorhodopsin,[4,5] and cytochrome C oxidase.[6,7] Photosynthetic reaction centers (RC) convert photochemical energy into electrochemical energy. They contain two symmetrically arranged subunits (L and M) with five TM-helices each (LA to LE, MA to ME) and an H subunit with a single TM-helix (HA) (Fig. 1).[8,9] The TM-helices adjacent in sequence tend to be neighbors in the structure; thus, the majority of pairwise helix–helix interactions are antiparallel. Yeates et al.[10] found that the sidechain packing within the RC TM-domain is as compact as in the hydrophobic cores of water-soluble proteins. Bacteriorhodopsin (BR) functions as a light-driven proton pump. It contains seven TM-helices (A to G) which form a hydrophilic pocket holding the covalently bound retinal chromophore and the proton channel. These helices are connected by short linkers and arranged in an antiparallel up-and-down topology (Fig. 1). BR's TM-helices are also densely packed; only a few cavities are found between them and are mainly restricted to the proton channel and the site of the retinal chromophore.[5] Cytochrome C oxidase (COX) is the terminal oxidase of cell respiration. The enzyme from beef heart mitochondria is composed of 13 different subunits, 10 of which are transmembrane.[7] Subunit III (COX_{III}), which was analyzed here, contains seven TM-helices; their pairwise interactions are mostly antiparallel.

The TM-helices of some other membrane proteins, e.g., the various light-harvesting centers, make no or only limited contact with each other due to the abundance of low-molecular weight cofactors binding to them.[11,12]

Since the database of high-resolution membrane protein structures is so small, detailed analyses of helix–helix packing have focused on soluble proteins. There, the long axes of interacting helices prefer either right-handed crossing angles at around -50° or left-handed angles at around +20°.[13–15] Helices interacting at left-handed angles are found within

Contract grant sponsor: Deutsche Forschungsgemeinschaft; Contract grant number: La699/4-1 (and HEISENBERG Programm); Contract grant sponsor: Fonds der Chemischen Industrie.
*Correspondence to: Dr. Dieter Langosch, Neurobiologie Department, Universität Heidelberg, Im Neuenheimer Feld 364, 69120 Heidelberg, Germany. E-mail: langosch@sun0.urz.uni-heidelberg.de
Received 7 April 1997; Accepted 31 October 1997

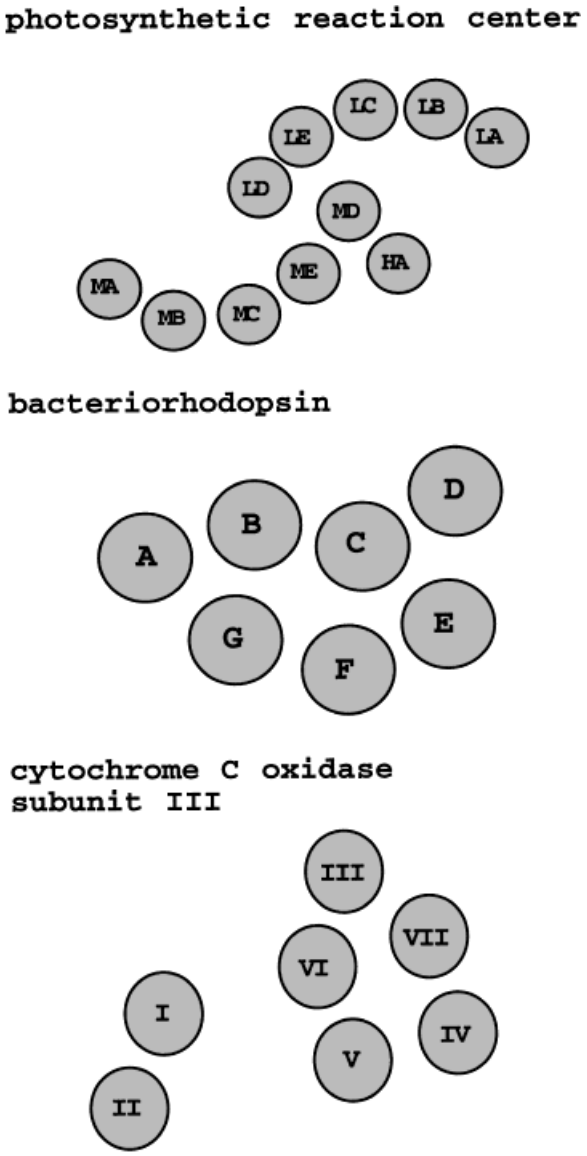

Fig. 1. Top view of the principal organization of the membrane-embedded helical bundles of the RC, BR, and COX_{III}. Helices are depicted as circles.

transcription factors of the bZIP family, in many fibrous proteins, and enzymes.[16–18] The left-handed interaction involves a two- to five-stranded bundle where the long helix axes assume a superhelical twist resulting in a coiled coil. The sidechains of one helix protrude into cavities formed by sidechains of the neighboring helix(es) in a regular manner which is termed knobs-into-holes or leucine zipper packing.[19–21] The interacting residues form a repeated motif of seven amino acids (*abcdefg*). The *a* and *d* positions are usually occupied by nonpolar residues constituting the hydrophobic core of the helix–helix interface; residues at the peripheral positions *e* and *g* are frequently charged and form salt-bridges to each other as well as hydrophobic contacts to the core residues.[22–25]

Similar to the coiled coils of soluble proteins, most TM-helices of the RC, BR, and COX are tilted relative to each other at left-handed angles ranging from 2° to 67° for the RC[9] and from 6° to 25° for BR.[5] Based on visual examination, these left-handed helix–helix pairs were proposed to follow a sidechain packing similar to coiled coils.[9,16,26–28] In the present study, we present a quantitative investigation of the packing between TM-helices done by a nearest-neighbor analysis of residues. The results corroborate that the basic geometry of left-handed helix–helix packing is conserved between membrane-embedded and soluble proteins and allow comparisons of the compactness of packing and the identity of interfacial residue types.

METHODS

Nearest-Neighbor Analysis

The nearest-neighbor analyses were performed using the program CLUSPROT, which is also available in interactive mode at http://www.embl-heidelberg.de/argos/clusprot/clusprot_info.html. The algorithm regards every residue having a main- or sidechain atom within 0.45 nm of the residue under consideration as a neighboring residue. This cutoff distance had previously proven suitable to identify sidechain clusters in soluble proteins.[29,30] Based on the number of sidechain atom–atom contacts thus identified, a quantitative measure of contact is defined and normalized to avoid bias toward large residues. The normalization values represent the maximal packing observed for each amino acid type over a large nonredundant set of soluble globular protein structures.[29] The normalized values are denoted pairwise contact percentage (PCP). The dense neighborhood threshold was set to 0.0% to retrieve all contacts identified by the program. For the present analyses, the atomic coordinates of the RC from *Rhodopseudomonas viridis* (PDB entry 1prc, 0.23 nm resolution[3]), BR from *Halobacterium halobium* (2brd, 0.35 nm resolution[5]), COX_{III} from beef heart (1occ, 0.28 nm resolution[7]), the GCN4 leucine zipper interaction domain from yeast (2zta, 0.18 nm resolution[21]), seryl tRNA synthetase from *Thermus thermophilus* (1ses, 0.25 nm resolution[31]), and ROP protein from *Escherichia coli* (1rop, 0.17 nm resolution[32]) were analyzed. Contacting residue pairs were manually extracted for each pair of adjacent TM-helices from the lists describing all residue–residue pairs. The residues pertaining to the individual helix–helix interfaces were marked on the sequences of the helices. The positions of the helices within the primary structures were taken from the publications cited above.

In the majority of cases, the set of residues contacting a given neighbor helix could be unambiguously assigned to a unique heptad repeat pattern by best

fit. In some cases, the cutoff distance had to be raised to identify additional residue–residue contacts allowing unambiguous assignments. For the RC, these are the following pairs: LC/LB (0.50 nm identified one more contact in LC), LE/LC (0.55 nm identified two more contacts in LE), MB/MC (0.60 nm identified one more contact in MC), as well as MD/HA (0.65 nm identified one more contact in MD). With the pairs LD/MD and LE/MD, assignments were ambiguous at all cutoff distances tested (0.40 to 0.65 nm). In these cases, those residues were assigned to *a*, *d*, *e*, *g* positions which exhibited the maximal sum of PCPs (i.e., maximal packing) over the whole interacting surfaces. Since too few contacts scored for the pair LC/MD up to 0.65 nm, no clear assignment of residues to a heptad repeat pattern could be made here. With COX_{III}, three additional residue–residue contacts were identified at a 0.65 nm cutoff distance for the pair of helices III and VI, thus allowing for an unambiguous assignment of the heptad repeat pattern. Three of the BR helices (B, C, F) contain proline residues and are therefore kinked by 16° to 24°.[5] With these helices, the contacting residues at either side of the kinks independently fit into the heptad motif but the motifs did not form uninterrupted repeat patterns over the whole lengths of the helices. Thus, gaps were inserted into the sequences close to the positions of the kinks to allow for the independent fits. In each case, the assignments resulted in interresidue connectivities predicted for knobs-into-holes packing.

Multiple Sequence Alignments

Sequences were aligned using the program MaxHom, which includes only homologs down to levels of 30% pairwise sequence identity over 80 or more residues (available at: http://www.emblheidelberg.de/predictprotein/predictprotein.html #PP1MAXHOM).[33] The alignment for the RC M subunit (SWISS-PROT accession number P06010) included homologs with the following accession numbers (pairwise sequence identities to the parent sequence in parentheses): P10718 (60%), P26279 (54%), P02953 (50%), P11847 (50%), PO9438 (39%). Alignment for the RC L subunit (P06009): P26280 (65%), P10717 (59%), P19057 (59%), P02954 (59%), P11695 (41%). Alignment for the RC H subunit (P06008): P11846 (39%), P19056 (39%). Alignment for BR (P02945): P19585 (57%), P29563 (56%), P33971 (56%), P33972 (55%), P33969 (55%), P42197 (36%), P16102 (34%), P33970 (33%), P15647 (33%), P33742 (31%), P42196 (31%), P33743 (30%). Alignment for COX_{III} (P00415): P14574 (71%), P00417 (65%), Q02654 (56%), P24891 (45%), P50677 (31%).

Compilation of Residue Type Distributions

Residue types found within the helix–helix interfaces of the analyzed structures were tabulated separately for *a*, *d*, *e*, or *g* positions. For an increased statistical weight of the tabulations, residue types at equivalent positions of aligned sequences of close homologs were also included. The relative frequency of occurrence of a residue type was defined as the percentage occurrence of a residue type at a particular heptad position divided by the general frequency of that residue type in proteins, as taken from Lupas et al..[34] In some cases, the same residue contributes to more than one interface and, consequently, was tabulated for each of the heptad positions they occupied. The frequencies of occurrence of residues in soluble coiled coils shown in Figure 5 is based on the numbers underlying the COILS program (available at: http://ulrec3.unil.ch/ coils/COILS_doc.html) and were kindly provided by Dr. Andrei Lupas.

RESULTS

The interfaces between the TM-helices of the RC, BR, and subunit III of COX (COX_{III}) were examined by a nearest-neighbor analysis of amino acids to 1) identify the interfacial residues, 2) assess the geometry and compactness of packing between the residues, and 3) compile the allowed types of interfacial amino acids.

Residues Involved in TM-Helix–Helix Interaction Are Part of a Heptad Motif

The recently refined coordinates of the RC, of BR, and those of mitochondrial COX formed the basis of the present study. For COX, only the second largest subunit III was chosen for the analysis as it contains a similar number of helix–helix interfaces as the RC and BR. The method of Heringa and Argos[29] was used to identify those residues contributing to the TM-helix–helix interfaces, as described in Methods. A given TM-helix participates in a number of interfaces equivalent to the number of neighboring helices in the structure. For each interface, contacting residue pairs were manually extracted from the list holding all residue–residue pairs of a structure. The positions of the residues associated with individual helix–helix interfaces were marked on the respective sequences. As exemplified by the helix–helix pair shown in Figure 2 (between helix MA and helix MB of the RC M subunit), most interfacial residues contact several other residues on a neighboring helix. Thus, meshworks of residue–residue contacts describing all helix–helix interfaces were identified. The marked sequences were then aligned for best fit with respect to the patterns of interfacial residues. Interestingly, the initial alignment immediately revealed that most interfacial residues occur at positions *a*, *d*, *e*, or *g* of a heptad repeat pattern. This is the motif which describes the helix–helix interfaces of left-handed coiled coils or leucine zipper interaction domains found in many soluble proteins. For the RC, 16 out of 22 patterns (corresponding to 12 interfaces) fit to unique repeats of the heptad motif. With some other interacting surfaces, the interfacial

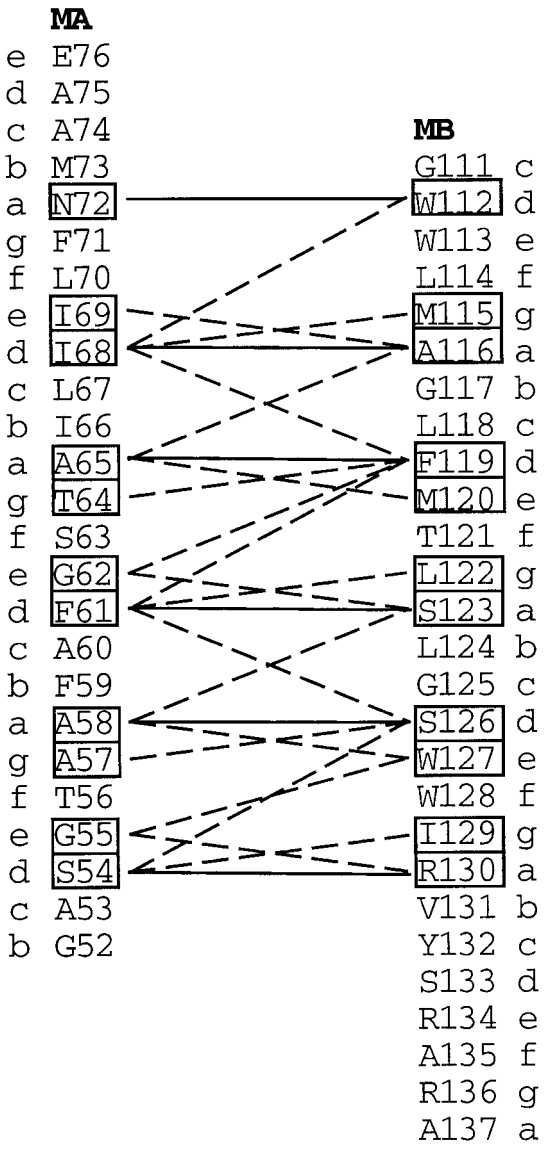

Fig. 2. Identification of residues contributing to helix–helix interfaces. In the example given, those residues of helices MA and MB of the RC which are close (≤0.45 nm) to one or more residues of the other helix are boxed. The assigned heptad repeat patterns are given next to the residues. Full lines connect *a* and *d* residues in the core of the helix–helix interfaces. Dashed lines connect all other residues.

residues identified at the cutoff distance of 0.45 nm fit into more than one unique heptad repeat pattern. However, unique assignments could be made after identifying additional contacts at cutoff distances up to 0.65 nm or by applying other criteria, as detailed in Methods. For BR, 7 out of 12 patterns could readily be assigned to unique heptad repeat patterns (considering only the left-handed pairs A/B, B/C, D/E, E/F, F/G, and G/A). Gaps had to be introduced into the sequences of the kinked helices B, C, and F to allow for unambiguous assignments of the residues interfacing helices C, B, and G, respectively, to the heptad motif. The two remaining patterns correspond to the right-handed pair of helices C and D and did not fit the heptad motif. For COX_{III}, 10 out of 14 patterns readily fit to unique heptad repeat patterns. Two additional patterns could be assigned after raising the cutoff distance to 0.65 nm and two patterns correspond to the right-handed pair of helices III and VII. Figure 3 shows the final alignment in which the interfacial residues identified at the 0.45 nm cutoff distance are boxed. For the RC, a total of 188 contacting residues occupy *a*, *d*, *e*, or *g* positions of the heptad motif (boxed and shaded); in addition, six residues were found which did not fit into this motif (only boxed). For BR, these numbers were 119 and 3 residues, and for COX_{III} they are 136 and 4 residues, respectively (not considering right-handed helix–helix pairs).

Thus, 97% of all residues identified within the left-handed TM-helix–helix interfaces conform to the heptad repeat pattern characteristic of soluble coiled coils. The interacting surfaces are extended over 16.2 ± 4.5 residues (mean ± SD) for the RC, 20.1 ± 1.5 residues for BR, and 21.5 ± 4.0 residues for COX_{III}, i.e., they contain between two and three heptad repeats.

As a control, the algorithm was applied to three representative soluble left-handed parallel or antiparallel coiled coils contained within the yeast nuclear transcription factor GCN4,[21] *T. thermophilus* seryl tRNA synthetase[31] and *E. coli* ROP protein.[32] In all three cases, the 0.45 nm cutoff distance correctly identified the interfacial residues at *a*, *d*, *e*, or *g* positions without outliers (Fig. 3). This confirms that the nearest-neighbor method is well suited to identify the residues participating in coiled coil type helix–helix interactions.

Knobs-Into-Holes Packing Describes the Interaction Between Transmembrane Helices

Within left-handed coiled coils in soluble proteins, the sidechains at positions *a* and *d* make up the hydrophobic core of the helix–helix interface. Each of these sidechains (knobs) pack into cavities (holes) surrounded by four sidechains of the neighbor helix. Thus, in parallel pairs residue *a′* on one helix packs against residues *a*, *d*, *d*, *g* of the neighbor and *d′* packs against *d*, *a*, *a*, *e*. In antiparallel pairs, *a′* packs against *d*, *a*, *a*, *e*, and *d′* packs against *a*, *d*, *d*, *g* (Fig. 4a). An examination of the residue–residue connections found within the interfaces of the TM-helices revealed that they follow this pattern very well (see Fig. 2, for example). For the RC, BR, and COX_{III} together, 96% (528 out of a total of 551) of all connections made by residues at *a* and *d* positions to residues of a neighbor helix conform to the knobs-into-holes scheme. For a quantitative estimate of the compactness of packing, a measure was derived from the PCPs exhibited by *a*- or *d*-type residues for their

different partners. These values were added up for *a*- and *d*-type residues of each helix–helix interface and divided by the number of *adeg*-type residues within the respective interface. The resulting values are denoted PCP/residue and were calculated either with or without the few contacts which did not conform to the knobs-into-holes connectivity. Finally, the PCP/residue values for the different helix–helix interfaces were averaged for each structure (Fig. 4b). It was found that the compactness of packing thus defined is similar around *a*- and *d*-type residues with all three membrane proteins and tends to be below that of the soluble coiled coils of GCN4, seryl tRNA synthetase, and ROP protein. Contacts which do not conform to the knobs-into-holes connectivity make small contributions to the helix–helix interfaces with all membrane proteins (Fig. 4b, black parts of bars) but were not found with the soluble coiled coils, as stated above.

Together, these results imply that a knobs-into-holes type of packing is well suited to describe the interaction of left-handed TM-helix–helix pairs. Compared to soluble coiled coils, helix–helix packing in the membrane proteins appears, however, somewhat less compact and less regular.

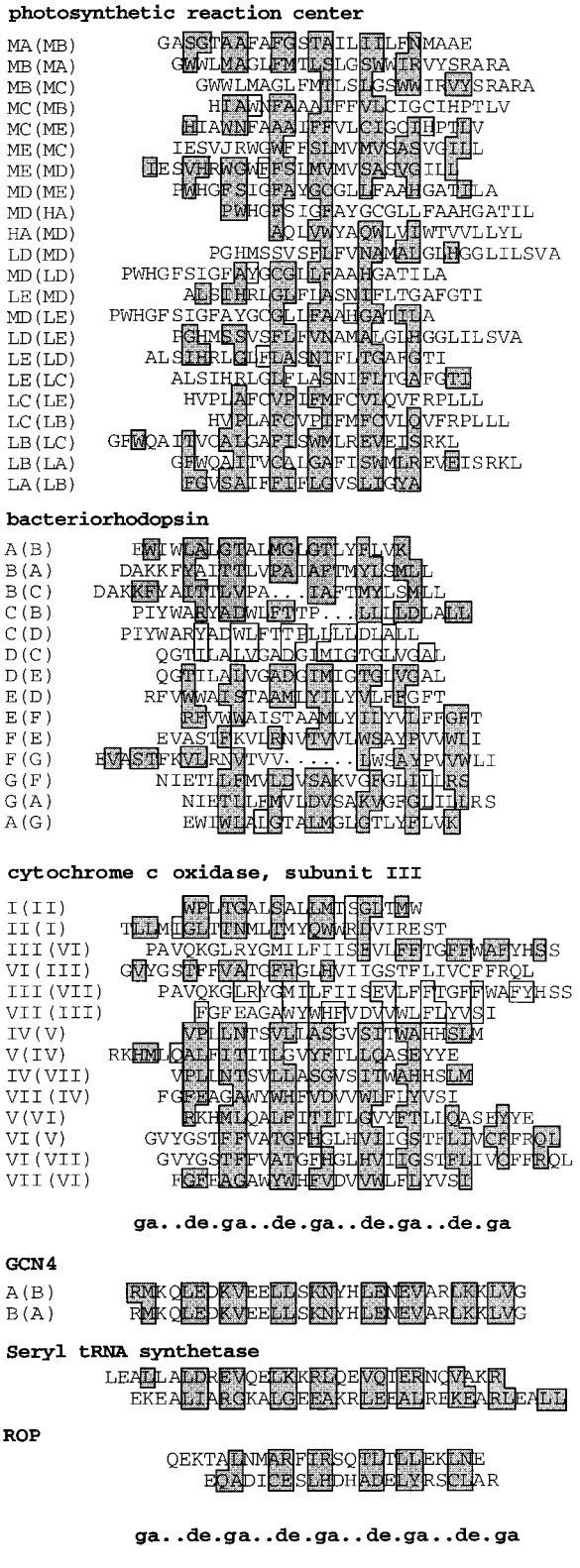

Fig. 3. Alignment of interfacial residues. The TM-helices of the RC, BR, and COX_{III} are compared to soluble coiled coils contained within the GCN4 leucine zipper interaction domain, seryl tRNA synthetase, and ROP protein. For a given helix, the number of marked sequences corresponds to the number of its different neighbor helices in the structure. Residues found to contact at least one residue on the neighbor helix under consideration (given in parentheses) at a 0.45 nm cutoff distance are boxed. Those residues at *a*, *d*, *e*, or *g* positions of the assigned heptad repeat pattern are shaded in addition. Dots inserted into the sequences of helices B, C, and F of BR denote gaps required to fit the contacting residues into a heptad motif at either side of the kinks made by these helices (see text for details). Note that C(D) and D(C) of BR as well as III(VII) and VII(III) of COX_{III} are part of right-handed helix–helix pairs.

Interfacial Positions Tolerate All Hydrophobic Residues Similarly

Here, it was determined whether the interfacial positions prefer certain amino acids. Residue types were tabulated separately for all the *a*, *d*, *e*, and *g* positions identified in the RC, BR, and COX_{III}. To increase the statistical weight of the resulting distributions, the residue types occurring at equivalent positions of homologous polypeptides were included. These were taken from multiple sequence alignments, including homologs down to levels of 30% pairwise sequence identity over 80 or more residues. This cut-off is five percentage points above the threshold for structural homology and the aligned residues are therefore likely to occupy equivalent positions in the different structures.[33] Finally, the distributions were normalized to the overall frequency of occurrence of the residue types in all proteins yielding their relative frequencies. These are visualized separately for the RC, BR, and COX_{III} in Figure 5 and averaged for all three structures in

Table I. The following results were obtained. 1) As expected for membrane-embedded domains, all positions strongly prefer hydrophobic residues (L, I, V, M, F, Y, W, C, A) plus glycine, serine, and threonine over hydrophilic and charged ones (H, Q, N, K, R, E, D). 2) Interestingly, tryptophan appears to be overrepresented within the TM-helix–helix interfaces of all three structures. 3) With respect to other hydrophobic residue types, *a*, *d*, *e*, and *g* positions do not exhibit preferences which would be conserved between the RC and BR. 4) Glycine occurs as frequently as the hydrophobic amino acids and more often than in soluble coiled coils. With the exception of tryptophan, these distributions are similar to the probabilities of the residue types to occur in TM-segments in general,[35,36] i.e., there seems to be little preference of interfacial positions for particular amino acid types. In contrast, previously calculated results showed that the *a* and *d* positions of soluble coiled coils prefer nonpolar residues (L, I, V, M, A, F, Y), whereas *e* and *g* positions prefer polar residues (Q, N, K, R, E, D)(Fig. 5).[34]

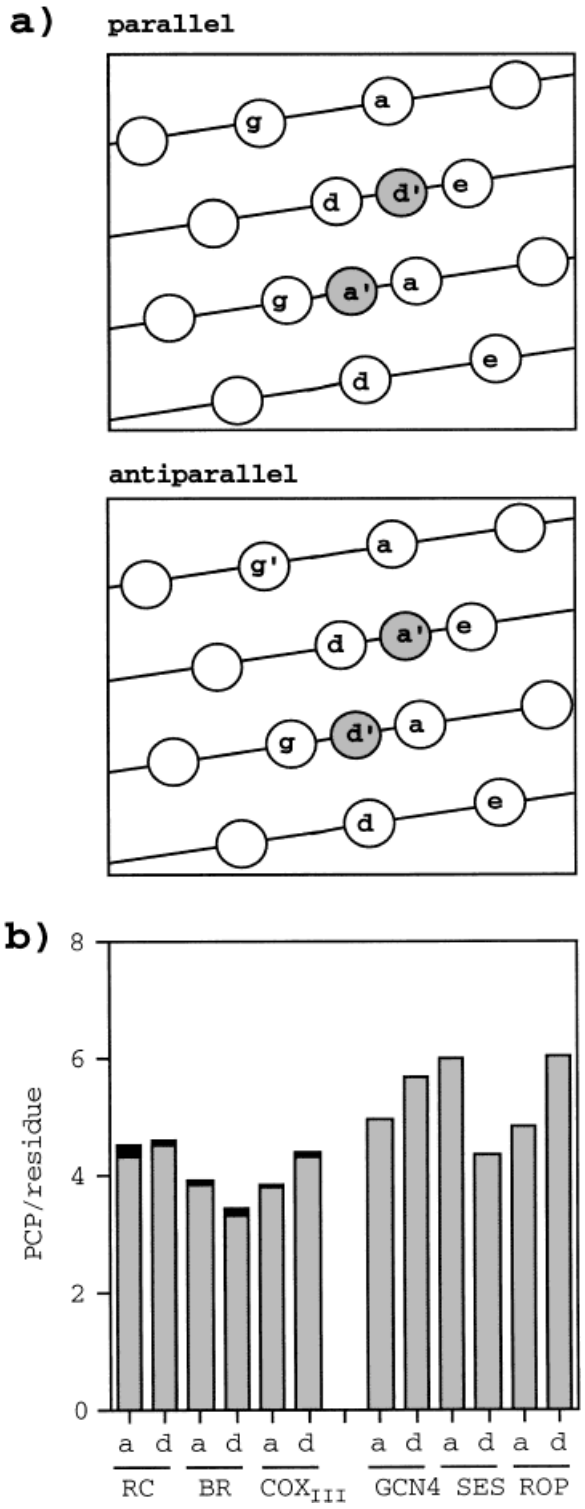

Fig. 4. Knobs-into-holes packing of left-handed helix–helix pairs. **a**: Schematic outline of the sidechain interactions describing the interfaces of parallel and antiparallel soluble coiled coils. Residues at *a′* or *d′* positions of one helix (shaded) pack into cavities formed by the sidechains of *a*, *d*, *e*, and *g* residues of the partner helix. **b**: Compactness of packing between TM-helices of the RC, BR, and COX_{III} compared to that of soluble coiled coils of the GCN4 leucine zipper, seryl tRNA synthetase (SES), or ROP protein. The compactness of packing was calculated separately around *a*- and *d*-type residues as detailed in the text. Contacts which do not fit the knobs-into-holes scheme were treated separately. They gave small extra contributions to helix–helix packing with the TM-helices (in black) but were not found for the soluble coiled coils.

DISCUSSION

To analyze the geometry of sidechain packing between TM-helices, a nearest-neighbor analysis of amino acids of the membrane-embedded α-helical bundles of the RC, BR, and COX_{III} was performed. The results demonstrate that the residues constituting the interfaces between left-handed pairs of TM-helices almost exclusively occupy positions *a*, *d*, *e*, or *g* of a heptad motif. This motif is repeated two to three times and any given TM-helix displays as many heptad repeat patterns as it has neighbors in the bundle. The vast majority of residue–residue contacts conforms to a knobs-into-holes type of packing characteristic of the coiled coil domains or leucine zippers found in many soluble proteins. Thus, the results corroborate on a quantitative basis earlier reports suggesting a similar organization of the α-helical TM-domains of BR or the RC and soluble coiled coils.[9,16,26–28] It is presently not clear whether interacting TM-helices form the superhelical twists which are known to maximize packing in soluble coiled coils. Previous results obtained with the RC, however, indicate a slight overwinding of its TM-helix backbones, which is consistent with formation of superhelical structures.[9]

The packing of sidechains within the TM-helical bundles tends to be somewhat less compact and less regular than that of soluble coiled coils analyzed in parallel. This conclusion is based on the observation that 1) the average PCP/values, which are based on

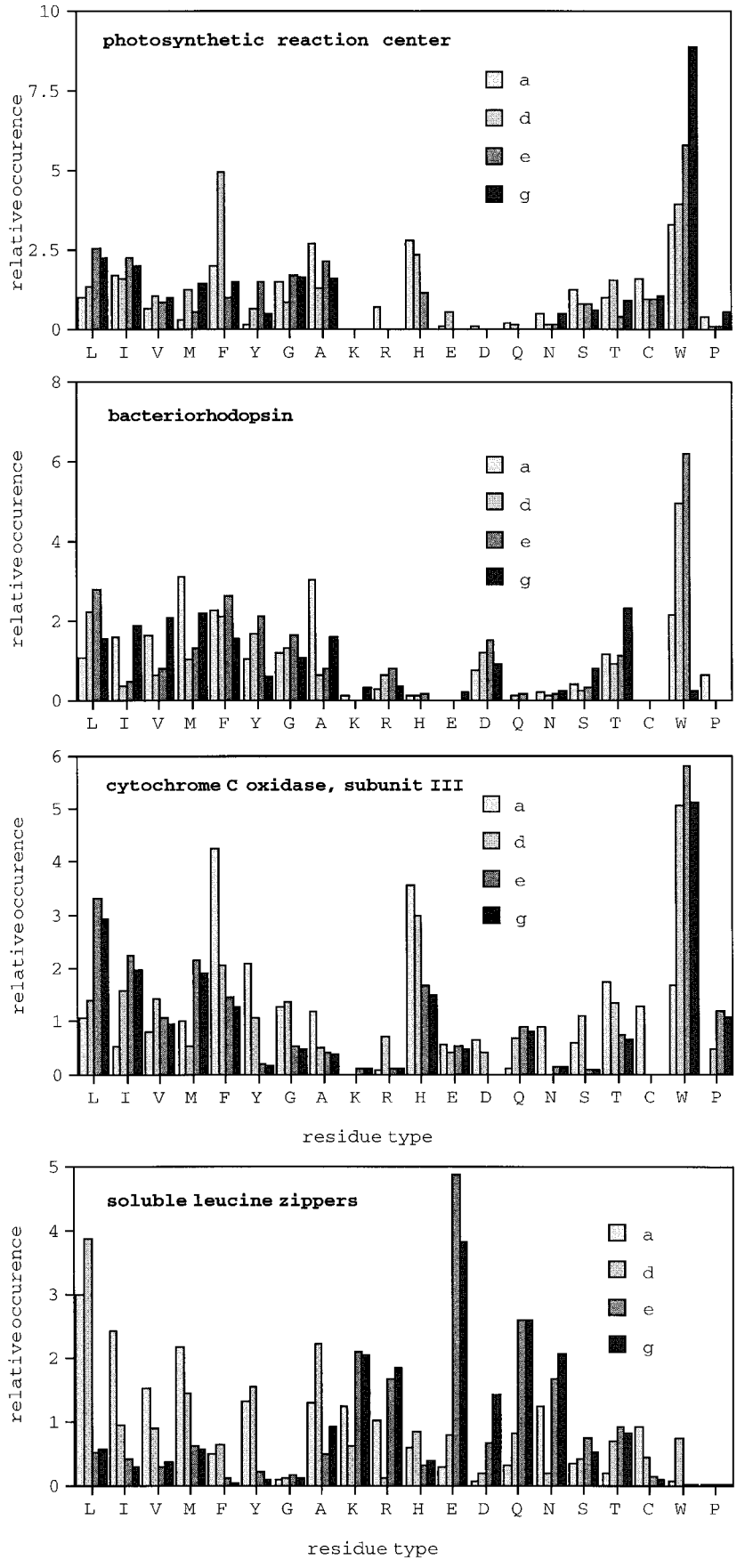

Fig. 5. Relative frequencies of occurrence of amino acid types at interfacial positions. The types of amino acids found in the helix–helix interfaces were tabulated separately for *a, d, e,* and *g* positions together with residues found at equivalent positions in homologous sequences. Relative frequencies of occurrence were calculated as detailed in Methods. These values indicate how much more (>1) or less (<1) often a residue occurs at a given position than in proteins in general. For comparison, the amino acid distribution previously found for soluble coiled coils is shown.

TABLE I. Relative Frequency of Occurrence of Residues Within Left-handed TM-Helix–Helix Interfaces

	Relative occurrence			
	a	*d*	*e*	*g*
L	1.01	1.71	2.80	1.59
I	1.36	1.20	1.41	1.79
V	1.10	1.11	0.85	1.64
M	1.67	1.68	1.23	1.89
F	2.61	3.03	1.84	1.96
Y	0.96	1.43	1.47	0.70
G	1.29	0.67	1.39	1.19
A	2.48	0.99	1.14	1.57
K	0.04	0.30	0.02	0.19
R	0.36	0.60	0.38	0.15
H	1.79	1.52	0.79	0.06
E	0.14	0.44	0.11	0.09
D	0.50	0.16	0.68	0.41
Q	0.08	0.21	0.26	0.16
N	0.44	0.14	0.13	0.52
S	0.70	0.87	0.40	0.74
T	1.22	1.41	0.78	1.83
C	0.82	0.43	0.29	0.74
W	2.39	5.13	5.93	3.05
P	0.39	0.34	0.29	0.16

the number of atom–atom distances at ≤0.45 nm, are somewhat smaller for TM-helix pairs than for soluble coiled coils, and 2) some residue–residue contacts within TM-helix–helix interfaces do not conform to the knobs-into-holes connectivity which describes soluble coiled coils. A non-optimal packing of TM-helices may allow for a certain flexibility required for protein function. For example, recent reports indicate that small movements of TM-helices relative to one another occur after light-activation of rhodopsin.[37,38]

The distribution of residue types at *a*, *d*, *e*, and *g* positions is markedly different between TM-helix interfaces and those of soluble coiled coils. Within the latter, the *a* and *d* positions of the hydrophobic core of the interface prefer nonpolar sidechains, whereas hydrophilic and charged residues predominate at *e* and *g* positions.[16,34] Ionic interactions between *e* and *g* positions may 1) stabilize helix–helix interaction,[24,25,39] 2) confer the specificity required for heteromeric assembly,[40] 3) shield the hydrophobic cores from water and the hydrophobic cores of other helix–helix pairs,[25] and/or 4) define parallel vs. antiparallel orientation of the interacting helices.[41] In contrast, the hydrophobic cores of helix–helix pairs located within lipid bilayers need not be shielded from their environment, but may interact with other helices to direct assembly of the complete bundles during folding. Consequently, charged sidechains at *e* and *g* positions are neither required nor would they be tolerated well in the hydrophobic environment of the membrane. Moreover, there would be no energetic penalty for large hydrophobic sidechains, such as that of the overrepresented tryptophan, to bulge out from the helix–helix interfaces.

There is increasing experimental evidence that specific interactions between TM-helices are a major driving force for correct folding and/or oligomerization of integral membrane proteins. This was initially suggested by the observation that separate fragments of bacteriorhodopsin or related molecules can be generated by cleaving linkers between TM-segments and subsequently be reconstituted to functional proteins.[28,42] This demonstrated that specific interactions between their TM-segments can specify their assembly. Further, a variety of bitopic oligomeric membrane proteins including glycophorin A,[43–45] the T-cell receptor,[46] the MHC-II complex,[47] the M13 major coat protein,[48] phospholamban,[49,50] synaptobrevin/VAMP II,[51] and others oligomerize via interactions between their respective TM-segments.[28] For the case of the phospholamban homopentamer, mutagenesis data and model building implied that interaction between its TM-helices involves a pattern of residues which conforms to the heptad motif characteristic of left-handed coiled coils.[49,50,52] Thus, the geometry of sidechain packing generating the phospholamban TM-helix bundle is equivalent to that found within the RC, BR, and COX_{III} in the present study. In contrast, right-handed pairs of TM-helices were implied in dimerization of glycophorin A and synaptobrevin/VAMP II on the basis of mutagenesis data.[43,51] For glycophorin A, this type of helix–helix pairing was recently confirmed by the solution NMR structure of its TM-domain.[53] Right-handed pairs of TM-helices are also found in the low-resolution structures recently reported for the aquaporin channel.[54,55]

CONCLUSION

Similar to the helices of soluble proteins,[13–15] left- and right-handed crossing angles appear to be alternative ways to maximize close packing of sidechains between interacting TM-helices. The predominance of left-handed helical pairs in the RC, BR, and COX suggests, however, that the knobs-into-holes geometry underlying left-handed crossing angles may be the more widespread mechanism of TM-helix–helix recognition.

ACKNOWLEDGMENTS

We thank Dr. Andrei Lupas for providing the frequencies of occurrence of amino acid types within soluble coiled coils and for critically reading the manuscript. We also thank Dr. Mathew Hannah for critically reading the manuscript, Rico Laage for stimulating discussions, and W.B. Huttner for continuous support. Work initiating this paper was done at the Laboratory for Molecular Biology in Cambridge, England.

REFERENCES

1. Deisenhofer, J., Epp, O., Miki, K., Huber, R., Michel, H. Structure of the photosynthetic reaction center from the purple bacterium *Rhodopseudomonas virides*. Nature 318: 618–623, 1985.
2. Allen, J.P., Feher, G., Yeates, T.O., Komiya, H., Rees, D.C. Structure of the reaction center from *Rhodobacter sphaeroides* R-26: The protein subunits. Proc. Natl. Acad. Sci. USA 84:6162–6166, 1987.
3. Deisenhofer, J., Epp, O., Sinning, I., Michel, H. Crystallographic refinement at 2.3 A resolution and refined model of the photosynthetic reaction center from *Rhodopseudomonas viridis*. J. Mol. Biol. 246:429–457, 1995.
4. Henderson, R., Baldwin, J.M., Ceska, T.A., Zemlin, F., Beckmann, E., Downing, K.H. Model for the structure of bacteriorhodopsin based on high resolution electron cryomicroscopy. J. Mol. Biol. 213:899–911, 1990.
5. Grigorieff, N., Ceska, T.A., Downing, K.H., Baldwin, J.M., Henderson, R. Electron-crystallographic refinement of the structure of bacteriorhodopsin. J. Mol. Biol. 259:393–421, 1996.
6. Iwata, S., Ostermeier, C., Ludwig, B., Michel, H. Structure at 2.8 A resolution of cytochrome c oxidase from *Paracoccus denitrificans*. Nature 376:660–669, 1995.
7. Tsukihara, T., Aoyama, H., Yamashita, E., et al. The whole structure of the 13-subunit oxidized cytochrome c oxidase at 2.8 A. Science 272:1136–1144, 1996.
8. Deisenhofer, J., Michel, H. High-resolution structures of photosynthetic reaction centers. Annu. Rev. Biophys. Biophys. Chem. 20:247–266, 1991.
9. Rees, D.C., Chirino, A.J., Kim, K-H., Komiya, H. Membrane protein structure and stability: Implications of the first crystallographic analyses. In: "Membrane Protein Structure." White, S.H. (ed.). Oxford: Oxford University Press, 1994:3–26.
10. Yeates, T.O., Komiya, H., Rees, D.C., Allen, J.P., Feher, G. Structure of the reaction center from *Rhodobacter sphaeroides* R-26: membrane-protein interactions. Proc. Natl. Acad. Sci. USA 84:6438–6442, 1987.
11. Kühlbrand, W., Wang, D.N., Fujiyoshi, Y. Atomic model of plant light-harvesting complex by electron crystallography. Nature 367:614–621, 1994.
12. McDermott, G., Prince, S.M., Freer, A.A., et al. Crystal structure of an integral membrane light-harvesting complex from photosynthetic bacteria. Nature 374:517–521, 1995.
13. Chothia, C., Levitt, M., Richardson, D. Helix to helix packing in proteins. J. Mol. Biol. 145:215–250, 1981.
14. Reddy, B.V.B., Blundell, R.L. Packing of secondary structural elements in proteins. J. Mol. Biol. 233:464–479, 1993.
15. Walther, D., Eisenhaber, F., Argos, P. Principles of helix–helix packing in proteins: The helical lattice superposition model. J. Mol. Biol. 255:536–553, 1996.
16. Cohen, C., Parry, D.A.D. alpha-helical coiled coils and bundles: How to design an alpha-helical protein. Proteins 7:1–15, 1990.
17. Alber, T. Structure of the leucine zipper. Curr. Opin. Genet. Dev. 2:205–210, 1992.
18. Lupas, A. Coiled coils: New structures and new functions. Trends Biochem. Sci. 21:375–382, 1996.
19. Crick, F.H.C. The packing of α-helices. Simple coiled-coils. Acta Crystallog. 6:689–697, 1953.
20. McLachlan, A.D., Steward, M. Tropomyosin coiled-coil interactions: Evidence for an unstaggered structure. J. Mol. Biol. 98:293–304, 1975.
21. O'Shea, E.K., Klemm, J.D., Kim, P.S., Alber, T. X-ray structure of the GCN4 leucine zipper, a two-stranded, parallel coiled coil. Science 243:539–544, 1991.
22. Schmidt-Dörr, T., Oertel-Buchheit, P., Pernelle, C., Bracco, L., Schnarr, M., Granger-Schnarr, M. Construction, purification, and characterization of a hybrid protein comprising the DNA binding domain of the LexA repressor and the Jun leucine zipper: A circular dichroism and mutangenesis study. Biochemistry 30:9657–9664, 1991.
23. Zhu, B-Y., Zhou, N.E., Kay, C.M., Hodges, R.S. Packing and hydrophobic effects on protein folding and stability: Effects of beta-branched amino acids, valine and isoleucine, on the formation and stability of two-stranded alpha-helical coils/leucine zippers. Protein Sci. 2:383–394, 1993.
24. Yu, Y., Monera, O.D., Hodges, R.S., Privalov, P.L. Ion pairs significantly stabilize coiled-coils in the absence of electrolyte. J. Mol. Biol. 255:367–372, 1996.
25. Krylov, D., Mikhailenko, I., Vinson, C. A thermodynamic scale for leucine zipper stability and dimerisation specificity: e and g interhelical interactions. EMBO J. 13:2849–2861, 1994.
26. Henderson, R., Unwin, N. Three dimensional model of purple membrane obtained by electron microscopy. Nature 257:28–32, 1975.
27. Harris, N.L., Presnell, S.R., Cohen, F.E. Four helix bundle diversity in globular proteins. J. Mol. Biol. 236:1356–1368, 1994.
28. Lemmon, M.A., Engelman, D.M. Specificity and promiscuity in membrane helix interactions. Q. Rev. Biophys. 27:157–218, 1994.
29. Heringa, J., Argos, P. Side-chain clusters in protein structures and their role in protein folding. J. Mol. Biol. 220:151–171, 1991.
30. Heringa, J., Argos, P., Egmond, M.R., de Vlieg, J. Increasing thermal stability of subtilisin from mutations suggested by strongly interacting side-chain clusters. Protein Eng. 8:21–30, 1995.
31. Fujinaga, M., Berthet-Colominas, C., Yaremchuk, A.D. Refined crystal structure ot the seryl-tRNA synthetase from *Thermus thermophilus* at 2.5 angströms resolution. J. Mol. Biol. 234:222, 1993.
32. Banner, D.W., Cesareni, G., Tsernoglou, D. Crystallization ot the col E1 rop protein. J. Mol. Biol. 170:1059, 1983.
33. Sander, C., Schneider, R. Database of homology-derived structures and the structural meaning of sequence alignment. Proteins 9:56–68, 1991.
34. Lupas, A., Van Dyke, M., Stock, J. Predicting coiled coils from protein sequences. Science 252:1162–1164, 1991.
35. Persson, B., Argos, P. Prediction of transmembrane segments in proteins utilising multiple sequence alignments. J. Mol. Biol. 237:182–192, 1994.
36. Reithmeier, R.A.F. Characterization and modeling of membrane proteins using sequence analysis. Curr. Opin. Struct. Biol. 5:491–500, 1995.
37. Farrens, D.L., Altenbach, C., Yang, K., Hubbell, W.L., Khorana, H.G. Requirement of rigid-body motion of transmembrane helices for light activation of rhodopsin. Science 274:768–770, 1996.
38. Sheikh, S.P., Zvyaga, T.A., Lichtarge, O., Sakmar, T.P., Bourne, H.R. Rhodopsin activation blocked by metal-ion-binding sites linking transmembrane helices C and F. Nature 383:347–350, 1996.
39. Zhou, N.E., Kay, C.M., Hodges, R.S. The role of interhelical ionic interactions in controlling protein folding and stability. J. Mol. Biol. 237:500–512, 1994.
40. O'Shea, E.K., Lumb, K.J., Kim, P.S. Peptide 'velcro': Design of a heterodimeric coiled coil. Curr. Biol. 3:658–667, 1993.
41. Monera, O.D., Kay, C.M., Hodges, R.S. Electrostatic interactions control the parallel and antiparallel orientation of alpha-helical chains in two-stranded alpha-helical coiled-coils. Biochemistry 33:3862–3871, 1994.
42. Popot, J-L., deVitry, C., Atteia, A. Folding and assembly of integral membrane proteins. In: "Membrane Protein Structure." White, S.H. (ed.). Oxford: Oxford University Press, 1994:41–97.
43. Lemmon, M.A., Flanagan, J.M., Treutlein, H.R., Zhang, J., Engelman, D.M. Sequence specificity in the dimerization of transmembrane alpha-helices. Biochemistry 31:12719–12725, 1992.
44. Lemmon, M.A., Treutlein, H.R., Adams, P.D., Brünger, A.T., Engelman, D. A dimerization motif for transmembrane alpha-helices. Nat. Struct. Biol. 1:157–163, 1994.
45. Langosch, D.L., Brosig, B., Kolmar, H., Fritz, H-J. Dimerisation of the glycophorin A transmembrane segment in membranes probed with the toxR transcription activator. J. Mol. Biol. 263:525–530, 1996.

46. Manolius, N., Bonifacino, J.S., Klausner, R.D. Transmembrane helical interactions and the assembly of the T cell receptor complex. Science 249:274–277, 1990.
47. Cosson, P., Bonifacino, J.S. Role of transmembrane domain interactions in the assembly of class II MHC molecules. Science 258:659–662, 1992.
48. Deber, C.M., Khan, A.R., Zuomei, L., Joensson, C., Glibowicka, M., Wang, J. Val-Ala mutations selectively alter helix–helix packing in the transmembrane segment of phage M13 coat protein. Proc. Natl. Acad. Sci. USA 90: 11648–11652, 1993.
49. Arkin, I.T., Adams, P.D., MacKenzie, K.R., Lemmon, M.A., Brünger, A.T., Engelman, D.M. Structural organization of the pentameric transmembrane alpha-helices of phospholamban, a cardiac ion channel. EMBO J. 13:4757–4764, 1994.
50. Simmerman, H.K.B., Kobayashi, Y.M., Autry, J.M., Jones, L.R. A leucine zipper stabilizes the pentameric membrane domain of phospholamban and forms a coiled-coil pore structure. J. Biol. Chem. 271:5941–5946, 1996.
51. Laage, R., Langosch, D. Dimerization of the synaptic vesicle protein synaptobrevin/VAMP II depends on specific residues within the transmembrane segment. Eur. J. Biochem. 249:540–546, 1997.
52. Arkin, I.T., Rothman, M., Ludlam, C.F.C., et al. Structural model of the phospholamban ion channel complex in phospholipid membranes. J. Mol. Biol. 248:824–834, 1995.
53. MacKenzie, K.R., Prestegard, J.H., Engelman, D.M. A transmembrane helix dimer: Structure and implications. Science 276:131–133, 1997.
54. Cheng, A., van Hoek, A.N., Yeager, M., Verkman, A.S., Mitra, A.K. Three-dimensional organization of a human water channel. Nature 387:627–630, 1997.
55. Walz, T., Hirai, T., Murata, K., et al. The three-dimensional structure of aquaporin-1. Nature 387:624–627, 1997.